Lab on a Chip

PAPER

View Article Online
View Journal

Cite this: DOI: 10.1039/d5lc00204d

Development of on-chip cell domes using Ca-alginate hydrogel shells for non-adherent cell studies†

Shinji Sakai, *[a] Hiroyuki Fujiwara,[ab] Ryotaro Kazama, [ac] Riki Toita [bd] and Satoshi Fujita *[bde]

Cell domes are hemispherical microstructures comprising hydrogel shells that enclose cells within their cavities. They are approximately 500 and 300 μm in radius and height, respectively. Multiple domes can be fabricated in an array on a single glass plate to facilitate optical observations and provide a localised and stable environment for non-adherent cell studies. However, current limitations, such as cytotoxicity, reduced cell viability and complex fabrication strategies, hinder their advancements. Thus, we address these limitations by proposing a cell dome system based on calcium ion (Ca^{2+})-crosslinked alginate hydrogel shells anchored to glass plates. The fabrication process was significantly streamlined and improved compared to previously reported enzyme-mediated methods, rendering it more accessible for biomedical applications. The resulting cell domes exhibited excellent adhesion stability to glass plates, maintaining an adhesion rate of >90% following 168 h of incubation under cell culture conditions. Enclosed K562 cells, which represent a non-adherent erythroleukemia cell line, exhibited consistent viability (>95%) and a 14-fold increase in cell proliferation over 72 h. The hydrogel shell enabled reagents, such as calcein-AM and ethidium homodimer-1, to enter the dome from the external environment. In addition, reagents could be transferred to the enclosed cells from within the dome by pre-depositing them onto the glass prior to dome preparation. Our proposed Ca-alginate cell dome broadens the application of cell domes as a scalable and versatile platform for high-throughput drug screening and cellular analysis, offering precise control over non-adherent cell studies.

Received 27th February 2025,
Accepted 22nd May 2025

DOI: 10.1039/d5lc00204d

rsc.li/loc

Introduction

Recent advancements in cell-based microarray technologies have significantly improved the capabilities of high-throughput screening for drug discovery and cellular function analysis.[1–3] These platforms facilitate the rapid and localised evaluation of cellular responses while assessing different compounds and conditions. However, despite their effectiveness with adherent cells,[1,2] high-throughput screening platforms face significant limitations, particularly regarding positioning, media exchange and analysis, when applied to non-adherent cells such as haematopoietic and immune cells.[4] Non-adherent cells are crucial for exploring various biological processes, such as immune responses, haematopoiesis and cancer cell behaviour.[5–7] However, their lack of substrate adhesion limits their compatibility with conventional cell-based assays and complicates cell positioning, media exchange and long-term high-throughput analysis.

To overcome these challenges, we previously reported a cell dome microarray system containing non-adherent cells encapsulated within hemispherical hydrogel domes. These domes were approximately 500 and 300 μm in radius and height, respectively, and had a hydrogel shell thickness of 100 μm.[8–10] Because the domes were immobilised on a transparent glass plate, they provided a stable microenvironment for non-adherent cells and enabled controlled optical observations and manipulations. The system also facilitated media exchange, chemical exposure, washing and staining, thereby enabling high-throughput cellular imaging comparable to adherent cell assays.

We previously employed hydrogel shells that were fabricated using the horseradish peroxidase (HRP)-mediated

[a] Division of Chemical Engineering, Department of Materials Engineering Science, Graduate School of Engineering Science, Osaka University, 1-3 Machikaneyamacho, Toyonaka, Osaka, Japan. E-mail: sakai@cheng.es.osaka-u.ac.jp
[b] Biomedical Research Institute, National Institute of Advanced Industrial Science and Technology (AIST), 1-8-31 Midorigaoka, Ikeda, Osaka, 563-8577, Japan. E-mail: s-fujita@aist.go.jp
[c] Department of Industrial Chemistry, Tokyo University of Science, 6-3-1 Niijuku, Katsushika-ku, Tokyo 125-8585, Japan
[d] AIST-Osaka University Advanced Photonics and Biosensing Open Innovation Laboratory, AIST, 2-1 Yamadaoka, Suita, Osaka 565-0871, Japan
[e] Cellular and Molecular Biotechnology Research Institute, National Institute of Advanced Industrial Science and Technology (AIST), 1-1-1 Higashi, Tsukuba, Ibaraki 305-8566, Japan

† Electronic supplementary information (ESI) available. See DOI: https://doi.org/10.1039/d5lc00204d

crosslinking of polymeric phenolic hydroxyl groups.[8–12] Although this enzyme-based method provided structural stability and ensured long-term cell containment, it had significant limitations. First, it required hydrogen peroxide for crosslinking, which poses cytotoxic risks.[13,14] Second, strict control over the peroxide concentration and exposure time was necessary to maintain cell viability.[15,16] Finally, the fabrication process was relatively complex, thus hindering its scalability and reproducibility.

To address these limitations, we propose a novel cell dome system based on calcium ion (Ca^{2+})-crosslinked alginate hydrogels. Alginate is a polysaccharide derived from seaweed that is widely recognised for its biocompatibility and rapid gelation in the presence of Ca^{2+} under physiological conditions mild for cells.[17–19] Owing to these features, Ca-alginate hydrogels have been widely used for cell encapsulation, particularly in the form of hydrogel beads[20,21] and microcapsules[22–24] for both adherent and non-adherent cells. By using this approach, we aimed to eliminate the need for enzymatic crosslinking, minimise cytotoxicity, and simplify fabrication. First, hemispherical gelatin hydrogels containing Ca^{2+} were formed on a glass plate, which was then immersed in a sodium alginate solution. The diffusion of Ca^{2+} ions into the surrounding alginate solution induced gelation, yielding a robust hydrogel shell. The gelatin hydrogel was then removed *via* thermo-induced gel-to-sol transition, resulting in a stable Ca-alginate hydrogel dome (Fig. 1).

K562 cells, which represent a non-adherent erythroleukemia cell line commonly used as a model in haematological research, were employed to assess the functionality of the fabricated Ca-alginate hydrogel domes. Moreover, their viability and proliferation were measured. The glass plate base facilitated the imaging processes, enabling detailed optical observations of the cells within the domes. Finally, we explored the potential of these domes as platforms for functional cell analysis by examining the uptake of reagents supplied externally and internally. This study explores the potential for controlled reagent delivery and high-throughput applications in cell domes, positioning this technology as a scalable platform for biomedical and pharmaceutical research.

Experimental

Materials

Sodium alginate (I-1G, MW: ~70 000 Da; mannuronic acid/glucuronic acid (M/G) ratio: 0.65) and porcine skin gelatin (gel strength ~300 g Bloom, type A) were obtained from Kimica (Tokyo, Japan) and Sigma-Aldrich (St. Louis, MO, USA), respectively. 3-Aminopropyltriethoxysilane (APS)-coated glass plates (18 mm × 18 mm; thickness: 0.8 mm) featuring ring-shaped water-repellent patterns (inner diameter: 1 mm; outer diameter: 1.4 mm) arranged in a 6 × 6 array with 2.5 mm spacing were purchased from Matsunami Glass Ind., Ltd. (Osaka, Japan). Water-soluble carbodiimide (WSCD), *N*-hydroxysuccinimide (NHS) and ethidium homodimer-1 were purchased from the Peptide Institute Inc. (Ibaraki, Japan), Fujifilm Wako Pure Chemical Corp. (Osaka, Japan) and Thermo Fisher Scientific (Waltham, MA, USA), respectively. Calcein-AM and CytoRed were purchased from Dojindo (Kumamoto, Japan).

K562 cells, a human chronic myelogenous leukaemia cell line, were obtained from the Riken Bioresource Center Cell Bank (Tsukuba, Ibaraki, Japan) and cultured in RPMI 1640 medium supplemented with L-glutamine (Fujifilm Wako Pure

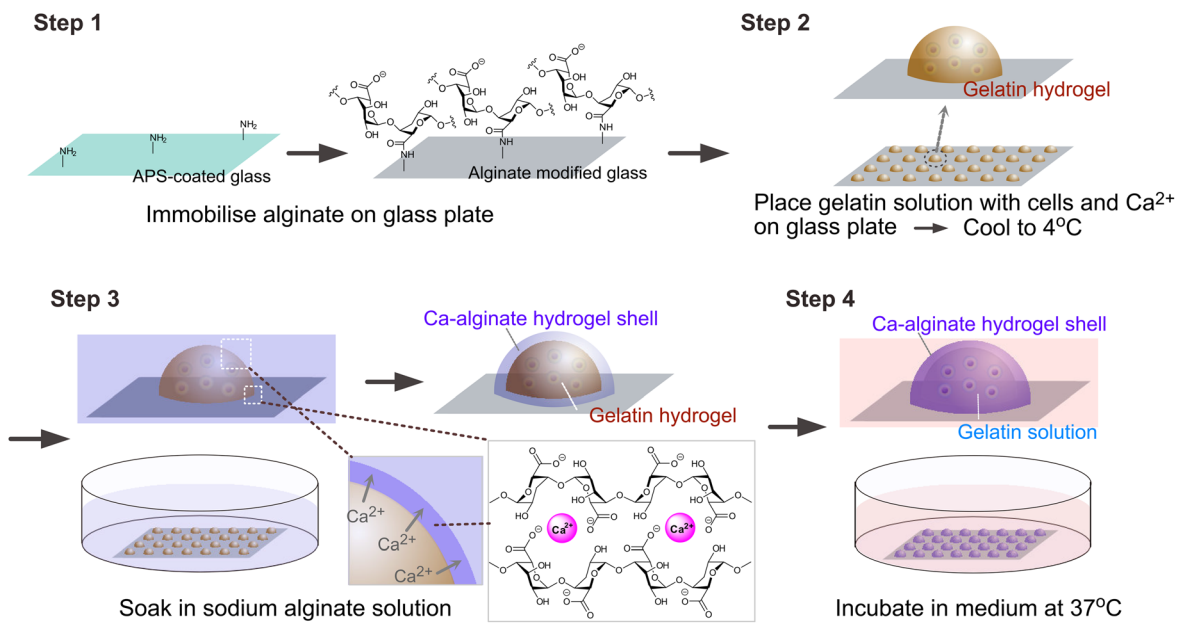

Fig. 1 Schematic illustration of the preparation of Ca-alginate hydrogel domes on a glass plate. Details of alginate immobilisation onto an APS-coated glass plate are provided in Fig. S1.†

Chemical Corp., Osaka, Japan), 10% foetal bovine serum (FBS; ICN Pharmaceuticals, Costa Mesa, CA, USA) and 1% penicillin–streptomycin (Nacalai Tesque, Kyoto, Japan).

Immobilisation of alginate on the APS-coated plate

Sodium alginate (1.2%, w/v) was first dissolved in 5 mL of 2-(*N*-morpholino)ethanesulfonic acid-buffered solution (pH: 6.0) and mixed with 1 mL of an aqueous solution containing 0.58% (w/v) WSCD and 0.17% (w/v) NHS. An APS-coated glass plate was immersed overnight in this mixture to facilitate carbodiimide crosslinking between the carboxyl groups of the alginates and the amino groups on the glass surface. Subsequently, the plate was rinsed with distilled water to remove any residual reagents and dried. The presence of alginate on the dried APS-coated glass plate was confirmed using X-ray photoelectron spectroscopy (XPS; Kratos Analytical Ltd., Manchester, UK) using an Al Kα source (1486.6 eV). An untreated APS-coated glass plate was used as the control.

Preparation of the alginate hydrogel dome array

Gelatin (1.6% w/v) was dissolved in 100 mM $CaCl_2$ solution at 37 °C. A 1 μL aliquot of this solution was dispensed onto the ring patterns (6 × 4 array) on the APS-coated glass plate. The plate was then stored at 4 °C for 10 min to induce cooling gelation. Following gelation, the glass plate with gelatin domes was immersed in a 0.5% (w/v) sodium alginate solution for 5 min, followed by rinsing with phosphate-buffered saline (PBS; pH: 7.4) and the cell culture medium. Cell-laden domes were prepared by incorporating K562 cells (2.1×10^5 cells per mL) into the gelatin solution prior to dispensing. The chemical characteristics of the Ca-alginate hydrogel formed on the gelatin hydrogel containing $CaCl_2$ domes were evaluated by FT-IR spectroscopy. The samples were freeze-dried prior to measurement. FT-IR spectra were recorded using a FT/IR-4100 spectrometer (JASCO, Tokyo, Japan) over the range of 4000–500 cm^{-1} with a resolution of 1 cm^{-1}. Sodium alginate was measured in the dried powder state as a reference.

Stability of the domes

Five sets of glass plates, each containing 24 cell-free domes, were immersed in a cell culture medium and incubated in a CO_2 incubator at 37 °C with 5% CO_2 and 95% air. The adhesion rate (%) was determined by counting the number of domains that remained attached to the substrate after 24, 48, 72 and 168 h. Control plates without alginate immobilisation were used for comparison.

Diffusion coefficients in the Ca-alginate hydrogel

Hydrogels were prepared by mixing 160 μL of 0.625% (w/v) sodium alginate solution with 40 μL of 500 mM $CaCl_2$ solution, resulting in a final composition of 0.5% (w/v) sodium alginate and 100 mM $CaCl_2$. The mixture gelated to form hydrogels with a composition comparable to that of the hydrogel shell. After washing twice with PBS, the hydrogels were immersed overnight at 37 °C in PBS containing 0.5 mg mL^{-1} fluorescein isothiocyanate-labelled dextran (FITC-dextran; molecular weight: 4000, 10 000 or 70 000 Da) purchased from Sigma-Aldrich (St. Louis, MO, USA). The diffusion coefficients of FITC-dextran in the hydrogel (D_{gel}) and water (D_{water}) were measured *via* fluorescence recovery after photobleaching using a confocal microscope, and the relative diffusion coefficients (D_{gel}/D_{water}) were calculated.

Cell culture and exposure to reagents supplied from outside the domes

Cell-laden domes on glass plates were immersed in the cell culture medium and incubated in a CO_2 incubator at 37 °C with 5% CO_2 and 95% air. At 24, 48 and 72 h, live and dead cells were stained with calcein-AM and ethidium homodimer-1, respectively. The phase-contrast and fluorescence images of the cells were acquired using an ECLIPSE Ti2-E microscope (Nikon, Tokyo, Japan).

Exposure to reagents delivered from within the cell dome

Poly(lactic-*co*-glycolic acid) (PLGA) was dissolved in dimethyl sulfoxide (DMSO) at 100 μg mL^{-1} and mixed in equal volume with DMSO containing 40 μM calcein-AM or 40 μM CytoRed. A 0.2 μL aliquot was dispensed onto each ring pattern on the alginate-modified glass plate, which were vacuum dried overnight to remove any solvent. Cell-laden alginate hydrogel domes were fabricated following the method described above, using a 1.6% (w/v) gelatin solution containing 100 mM $CaCl_2$ and 6.8×10^5 K562 cells per mL. The plates were placed in 35 mm culture dishes with 3 mL of medium and incubated in a CO_2 incubator for 24 h. The phase-contrast and fluorescence images of the cells were acquired.

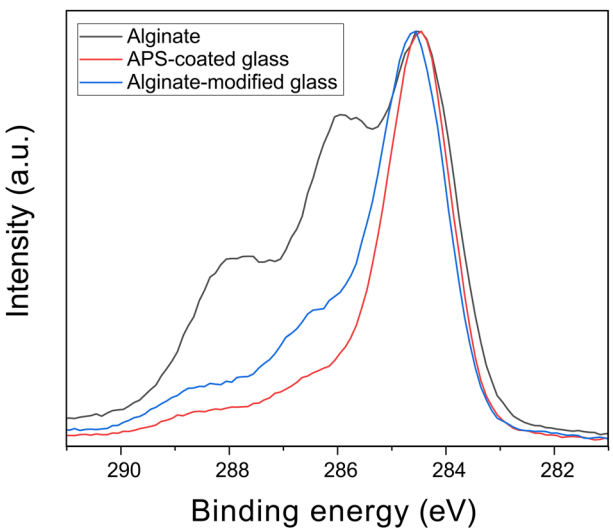

Fig. 2 XPS spectra of the sodium alginate powder (alginate), APS-coated glass (APS glass) and alginate-modified APS-coated glass (alginate-modified glass), illustrating the surface chemical composition.

Results

Fabrication and stability of the Ca-alginate hydrogel dome

Fig. 2 shows the XPS spectra of sodium alginate, the APS-coated glass plate and the APS-coated glass plate treated for immobilising alginate. The observed spectral differences confirmed the successful covalent modification of the APS-coated glass surface with alginate molecules. For example, the characteristic peak at approximately 288 eV, which corresponds to the C═O bond of carboxyl groups in alginate, was observed in the alginate-modified glass spectrum. This peak indicated the formation of covalent bonds between the alginate molecules and amino groups on the glass surface.

Fig. 3a shows the successful fabrication of multiple Ca-alginate hydrogel domes on the alginate-modified glass plate. The uniform arrangement of the domes confirmed the reproducibility of the fabrication process. Confocal laser fluorescence microscopy revealed the presence of a hemispherical cavity within the domes, with a cavity radius and height of 500 and 336 ± 42 μm, respectively, and a hydrogel shell thickness of 675 ± 30 μm. The chemical characteristics of Ca-alginate were also confirmed by FT-IR spectroscopy, using sodium alginate as a reference.

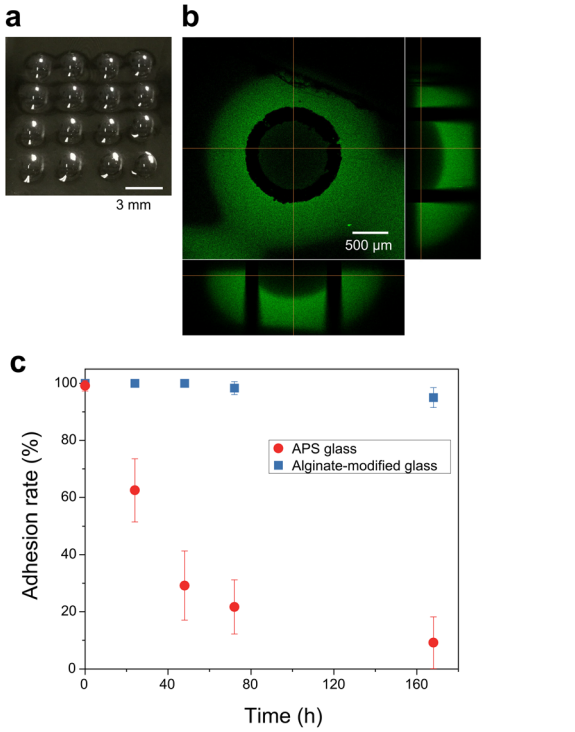

Fig. 3 a) Ca-alginate hydrogel domes prepared on an alginate-modified glass plate. b) Confocal laser fluorescence microscope image of the Ca-alginate cell dome obtained using FITC-labelled Na-alginate solution. c) Adhesion stability of Ca-alginate hydrogel domes on APS-coated glass plates (APS glass) and alginate-modified glass plates during 168 h of soaking in culture medium at 37 °C. The adhesion rate (%) was calculated as the percentage of domes that remained adhered over time. Data represent the mean ± S.D. (n = 5, independent experiments).

As shown in Fig. S2,† the FT-IR spectrum of Ca-alginate exhibited characteristic shifts in the asymmetric and symmetric COO^- stretching bands—from 1615 and 1417 cm^{-1} in sodium alginate to 1610 and 1424 cm^{-1}, respectively. These peak shifts are indicative of ionic crosslinking between carboxylate groups and calcium ions. These spectral features are consistent with previous reports on ionically crosslinked alginate.[25] Fig. 3c illustrates changes in the adhesion rate (%) of Ca-alginate hydrogel domes on the APS-coated and alginate-modified glass plates during 168 h of immersion in a medium in a CO_2 incubator at 37 °C. After 168 h, approximately 10% of the domes remained adhered to the APS-coated glass plates, whereas >90% remained on alginate-modified glass plates. Thus, the covalent immobilisation of alginate on the glass plate surface improved the stability of Ca-alginate hydrogel domes in the culture medium.

Diffusion coefficients in Ca-alginate hydrogel

The diffusion coefficients of FITC-dextran with molecular weights of 4000, 10 000 and 70 000 Da in the Ca-alginate hydrogel were 2.15 × 10^{-10}, 1.62 × 10^{-10} and 0.94 × 10^{-10} m^2 s^{-1}, respectively. These values represented 95%, 86% and 61%, respectively, of their respective diffusion coefficients in water (Fig. 4).

The size-dependent diffusion pattern was consistent with previous studies on Ca-alginate gels, where small molecules freely diffused and larger macromolecules were gradually restricted.[26,27]

Growth of K562 cells in the domes and exposure to reagents delivered from outside the domes

To evaluate the behaviour of K562 cells within the Ca-alginate cell domes, we monitored cell viability and growth over time using live/dead assays based on calcein-AM/ethidium homodimer-1 staining. Immediately after cell dome

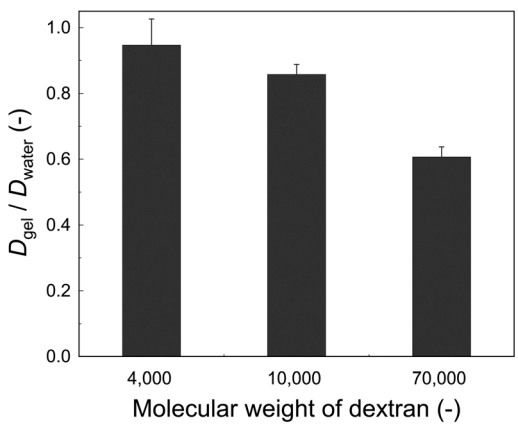

Fig. 4 Relative diffusion coefficients (D_{gel}/D_{water}) of FITC-dextran (MW: 4000, 10 000 and 70 000 Da) in Ca-alginate hydrogel, normalized by their diffusion coefficients in water. Diffusion coefficients were determined using FRAP. Data represent the mean ± S.D. (n = 5, independent measurements).

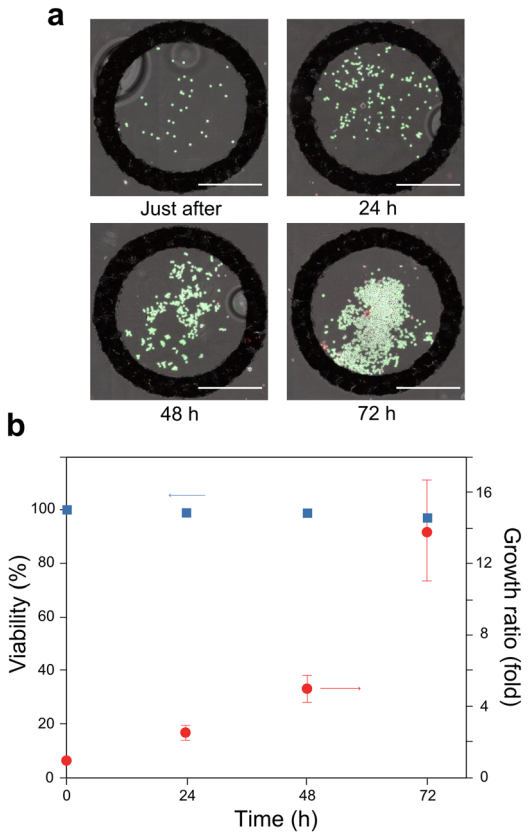

Fig. 5 (a) Merged bright-field and fluorescence microscopy images of K562 cells enclosed in a Ca-alginate hydrogel dome at different times. Live cells (green) and dead cells (red) were stained with calcein-AM and ethidium homodimer-1, respectively. Scale bar: 500 μm. (b) Viability (%) and growth ratio (fold increase) of K562 cells cultured within the Ca-alginate hydrogel domes over 72 h. The growth ratio was calculated relative to the initial number of cells enclosed in the domes. Data represent the mean ± S.D. (n = 8 for viability and n = 5 for growth ratio; independent experiments).

fabrication (Fig. 5a), nearly all the enclosed cells emitted a green fluorescent signal, confirming their viability. During the following 72 h of culture, the enclosed cells exhibited steady proliferation with only a minimal number of dead cells, as indicated by the red fluorescent signal. The quantitative analysis presented in Fig. 5b confirms these observations. Notably, cell viability remained >95% throughout the 72 h culture period, and cell growth steadily increased, reaching approximately 14-fold after 72 h.

The enclosed cells were successfully stained with calcein-AM and ethidium homodimer-1. Thus, the hydrogel shell enabled efficient reagent delivery for live cell imaging and functional analysis, highlighting its potential as a versatile platform for non-adherent cell studies.

Exposure of enclosed cells to reagent delivery from within the cell dome

To investigate the feasibility of the internal reagent supply, we utilised PLGA layers containing calcein-AM (green) and

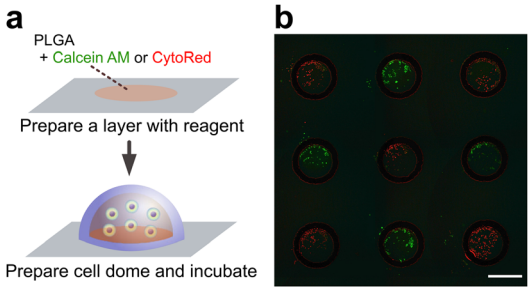

Fig. 6 (a) Schematic representation of the preparation of cell domes incorporating PLGA layers containing calcein-AM (green) or CytoRed (red), followed by the formation of Ca-alginate hydrogel domes. Fluorescent reagents were released from the PLGA layers and integrated into enclosed cells. (b) Merged bright-field and fluorescence microscopy image of the K562 cells after one day of incubation, demonstrating the intracellular uptake of fluorescent reagents. Scale bar: 1 mm.

CytoRed (red) at the dome base (Fig. 6a). After one day of incubation, fluorescence microscopy confirmed the localised distribution and uptake of the dyes within the enclosed cells (Fig. 6b). Notably, the fluorescence was negligible outside the domes, confirming that reagent delivery was spatially confined to the enclosed cells. These results demonstrated the successful localised delivery of reagents from the base layer to the enclosed cells.

Discussion

Ca-alginate hydrogels have attracted attention in the biomedical field owing to their mild gelation conditions, excellent biocompatibility and high molecular permeability.[17–19,28] They have also been widely used as beads[20,21] and microcapsules[22–24,29] for encapsulating cells without promoting adhesion. These features render them suitable for the shell of cell domes. In this study, we successfully fabricated stable Ca-alginate hydrogel domes by covalently immobilising alginate molecules onto APS-coated glass plates, thereby significantly enhancing their adhesion stability. Our previous work demonstrated that HRP-mediated hydrogel domes provided a stable environment for non-adherent cells.[8,10] However, hydrogen peroxide introduced potential cytotoxicity and required strict control over the reaction conditions. In contrast, the Ca-alginate hydrogel domes developed in this study eliminated the need for enzymatic crosslinking, reduced cytotoxicity and simplified the fabrication process.

Hydrogel-based platforms such as arrays,[30,31] microfluidic devices,[32] and microcapsules[24,29] have also been explored for non-adherent cell culture. While these systems enable spatial confinement or 3D encapsulation, they often lack reagent exchange capability, positional stability, or scalability. By contrast, our system forms hemispherical Ca-alginate domes immobilised on transparent substrates, allowing long-term proliferation of suspension cells, optical observation, and reagent delivery from both inside and outside. These features

make it a practical and versatile platform for high-throughput suspension cell studies.

Several alginate-based microarray systems have also been reported for screening and spatial patterning, using techniques such as inkjet spotting,[33] electrodeposition,[34] electrowetting,[35] or surface modification.[33,34,36,37] While these platforms enable spatially organised hydrogel structures, they typically produce flat or solid geometries and are not designed to support the long-term proliferation of suspension cells within confined three-dimensional environments. For instance, the hemispherical alginate spots reported by Richardson *et al.* were solid and lacked internal cavities that allow volumetric cell growth. In contrast, our system uniquely forms hollow, hemispherical hydrogel shells that are stably immobilised on glass substrates, providing spatial control, optical accessibility, and dual-mode reagent delivery, without requiring specialised fabrication techniques. To our knowledge, no previously reported alginate-based platform integrates these features into a single, scalable format suitable for suspension cell studies.

Stability of Ca-alginate hydrogel domes

Our initial experiments involved fabricating Ca-alginate hydrogel domes on APS-coated glass plates *via* electrostatic interactions between the carboxyl groups of the alginates and the amino groups on the glass surface. However, because this method did not provide sufficient stability for the cell domes, we exploited the covalent immobilisation of alginate molecules onto glass plates. This approach enabled crosslinking *via* Ca^{2+} between the immobilised alginate and hydrogel shell, retaining >90% of domes after 168 h of immersion in the culture medium (Fig. 3c).

Although this method demonstrated excellent stability, future improvements should be explored. Alternative crosslinking ions such as Ba^{2+} or Sr^{2+} exhibit strong affinities for alginate molecules, forming stable hydrogels under physiological conditions.[19,28] Additionally, using alginate with a higher glucuronic acid content could further enhance stability because Ca^{2+} preferentially binds to G- and MG-blocks, thus increasing the structural integrity of the hydrogel network.[19,28]

Molecular permeability and cytocompatibility

The Ca-alginate hydrogels possessed a porous structure that enabled the diffusion of small molecules while limiting the transport of larger macromolecules. The FITC-dextrans of 4000, 10 000 and 70 000 Da exhibited relative diffusion coefficients (D_{gel}/D_{water}) of 0.95, 0.86 and 0.61, respectively (Fig. 4). Thus, the size-dependent diffusion pattern observed in our study suggested that the hydrogel network effectively regulated molecular transport. Moreover, these findings align with those of previous studies on Ca-alginate gels, which have reported preferential permeability for small molecules while gradually restricting the diffusion of larger macromolecules.[26,27] The characteristics observed in this study are essential for maintaining a suitable microenvironment for non-adherent cell cultures because they ensure the sufficient exchange of oxygen, nutrients and metabolic byproducts.

The comparable doubling times of K562 cells within the domes (approximately 19.5 h) and under standard culture conditions (16–24 h) indicated that the molecular permeation characteristics of the Ca-alginate hydrogel shell were sufficient to support oxygen and nutrient diffusion while maintaining cytocompatibility. The successful delivery of staining reagents from outside the domes (calcein-AM and ethidium homodimer-1; Fig. 5a) demonstrated that cell domes with the Ca-alginate hydrogel shell were suitable for assessing cell behaviour and functionality. This finding is consistent with those of previous reports, demonstrating the possibility of staining encapsulated cells in Ca-alginate hydrogel microcapsules.[22]

Although our results confirmed that the hydrogel composition used in this study provided a balance between stability and permeability, further modifications should be carefully evaluated. For instance, replacing Ca^{2+} with Ba^{2+} or Sr^{2+} to improve stability may alter hydrogel porosity and molecular transport properties. Similarly, varying the M/G ratio, molecular weight and concentration of alginate could influence both the permeability and mechanical integrity. Therefore, when optimising hydrogel formulations for specific applications, simultaneously assessing both the stability and permeability is essential to ensure a well-balanced system.

Further optimisation of the hydrogel composition and crosslinking conditions could fine-tune the permeability while maintaining structural stability, thereby broadening its applicability in biomedical research.

Localised reagent delivery

Owing to the permeability characteristics of the Ca-alginate hydrogels (Fig. 4 and 5a), calcein-AM and CytoRed (MW < 1000 Da) were expected to diffuse outside the domes to a certain extent. However, the observed variations in the dye uptake between adjacent domes (Fig. 6b) demonstrated the potential to create distinct microenvironments within the arrayed domes. By incorporating different substances into the PLGA layer, this system allowed controlled reagent release, thus enabling diverse experimental conditions within a single platform.

For instance, one dome could release a growth factor to promote cell proliferation, while another could release a signalling inhibitor to examine cellular responses to external stimuli. This capability highlights the versatility of the system in investigating spatially distinct cellular behaviours under controlled conditions.

To further regulate molecular transport while maintaining cell viability, polyion complex layer(s) comprising cationic polymers such as poly-L-lysine[38,39] or chitosan[23,40] could be formed on the Ca-alginate hydrogel shell surface. This

approach has been widely employed in microencapsulation technologies for cell therapies, particularly to enhance immune isolation.

For reagents delivered to cells from the PLGA layer, a different approach was required for substances such as enzymes and antibodies that are deactivated by the organic solvents used to dissolve PLGA. Previous studies using cell domes with hydrogel shells fabricated *via* HRP-mediated crosslinking demonstrated the successful delivery of plasmid DNA enclosed in a thin gelatin layer obtained from an aqueous gelatin solution. This process facilitated the transfection of enclosed cells while minimising leakage or contamination.[9] Thus, these strategies highlight the versatility of the system for investigating spatially distinct cellular behaviours.

Limitations and future directions

Despite these promising results, several challenges need to be addressed. First, the current manual preparation of Ca-alginate hydrogel domes at the laboratory scale presents limitations regarding scalability and reproducibility, thus hindering industrial applications. The variability in dome size and hydrogel shell thickness, which are inherent to manual fabrication, may also affect experimental consistency and data reproducibility. To overcome these challenges, automating the preparation process using microfluidics or advanced fabrication techniques, such as 3D printing, could improve dome uniformity, throughput and batch-to-batch consistency. Additionally, integrating these techniques with real-time imaging and automated analysis systems could enhance the efficiency of high-throughput drug screening applications. Second, long-term stability data beyond 168 h remains lacking. Although our results demonstrated that Ca-alginate hydrogel domes maintained high adhesion stability for seven days, further studies are required to evaluate their mechanical integrity, hydrogel degradation and cell viability over extended culture periods, such as weeks and months. Gradual hydrolysis or ion exchange in physiological environments may alter the mechanical properties of the hydrogel shell, potentially affecting its suitability for long-term applications. Future investigations should assess these factors to optimise the hydrogel formulations for prolonged use. Finally, while our study focused on K562 cells, further research should explore the compatibility of Ca-alginate hydrogel domes with a broader range of cell types, particularly primary haematopoietic stem and immune cells, which often have stricter culture requirements.[41–44] The permeability and stiffness of the hydrogel shell may require adjustments to support the specific metabolic and mechanical needs of different cell types. Additionally, the effects of the Ca-alginate gelation conditions on sensitive cell populations should be evaluated to ensure robust cell viability and functionality.

By addressing these challenges, the Ca-alginate hydrogel dome system could be further refined into a highly versatile and scalable platform for biomedical and pharmaceutical research.

Conclusions

In this study, we developed a novel fabrication process for cell domes with Ca-alginate hydrogel shells immobilised on glass plates, greatly simplifying the previous HRP-mediated methods. The resulting cell domes exhibited excellent adhesion stability, cytocompatibility and permeability and supported the robust growth of non-adherent K562 cells over extended culture periods. The domes enabled the efficient delivery of reagents from external sources and pre-deposited layers, demonstrating their versatility for dynamic cell studies.

Compared to HRP-based hydrogel domes, the Ca-alginate hydrogel dome system significantly reduces cytotoxicity and simplifies fabrication, rendering it a promising alternative for high-throughput drug screening and non-adherent cell research.

Future studies should focus on optimising fabrication techniques, extending stability testing and broadening the compatibility with other cell types to enhance their impact on biomedical applications.

Data availability

The data supporting the findings of this study are available within the article.

Author contributions

Conceptualisation: S. S. and S. F.; methodology: S. S. and S. F.; formal analysis: H. F. and R. K.; investigation: H. F. and R. K.; resources: S. S. and S. F.; data curation: S. S. and S. F.; writing – original draft preparation: S. S. and S. F.; writing – review and editing: S. S., R. K., R. T. and S. F.; visualisation: S. S.; supervision: S. S. and S. F.; project administration: S. S. and S. F.; and funding acquisition: S. S. and S. F. All authors have read and agreed to the published version of the manuscript.

Conflicts of interest

There are no conflicts to declare.

Acknowledgements

This research was supported by the JSPS KAKENHI (grant numbers 24K22379 and JP17H03472). We would like to thank Editage (**https://www.editage.jp**) for English language editing.

Notes and references

1 H. Ryoo, H. Kimmel, E. Rondo and G. H. Underhill, *Bioeng. Transl. Med.*, 2024, **9**, e10627.
2 J. Sarkar and A. Kumar, *Biotechnol. J.*, 2021, **16**, e2000288.
3 J. Wegener, *Annu. Rev. Anal. Chem.*, 2015, **8**, 335–358.
4 S. Yamaguchi, E. Matsunuma and T. Nagamune, *Methods Mol. Biol.*, 2011, **706**, 151–157.
5 B. Cai, T. T. Ji, N. Wang, X. B. Li, R. X. He, W. Liu, G. Wang, X. Z. Zhao, L. Wang and Z. Wang, *Lab Chip*, 2019, **19**, 422–431.

6 A. Backstrom, L. Kugel, C. Gnann, H. Xu, J. E. Aslan, E. Lundberg and C. Stadler, *J. Histochem. Cytochem.*, 2020, **68**, 473–489.
7 V. E. Brett, F. Dignat George and C. James, *Curr. Opin. Hematol.*, 2024, **31**, 148–154.
8 R. Kazama, R. Sato, H. Fujiwara, Y. Qu, M. Nakahata, M. Kojima, S. Fujita and S. Sakai, *Biofabrication*, 2022, **15**, 015002.
9 R. Kazama, S. Fujita and S. Sakai, *Biochem. Eng. J.*, 2025, **213**, 109554.
10 R. Kazama, R. Ishikawa and S. Sakai, *Bioengineering*, 2024, **11**, 1303.
11 R. Kazama, S. Fujita and S. Sakai, *Cells*, 2022, **12**, 69.
12 R. Kazama and S. Sakai, *J. Biosci. Bioeng.*, 2024, **137**, 313–320.
13 S. Sakai and K. Kawakami, *Acta Biomater.*, 2007, **3**, 495–501.
14 S. Sakai, K. Hirose, K. Taguchi, Y. Ogushi and K. Kawakami, *Biomaterials*, 2009, **30**, 3371–3377.
15 M. Gulden, A. Jess, J. Kammann, E. Maser and H. Seibert, *Free Radical Biol. Med.*, 2010, **49**, 1298–1305.
16 W. H. Park, *Mol. Med. Rep.*, 2013, **7**, 1235–1240.
17 O. Smidsrod and G. Skjakbraek, *Trends Biotechnol.*, 1990, **8**, 71–78.
18 W. K. Abdelbasset, S. A. Jasim, S. K. Sharma, R. Margiana, D. O. Bokov, M. A. Obaid, B. A. Hussein, H. A. Lafta, S. F. Jasim and Y. F. Mustafa, *Ann. Biomed. Eng.*, 2022, **50**, 628–653.
19 Y. A. Morch, I. Donati, B. L. Strand and G. Skjak-Braek, *Biomacromolecules*, 2006, **7**, 1471–1480.
20 H. Onoe, K. Inamori, M. Takinouec and S. Takeuchi, *RSC Adv.*, 2014, **4**, 30480–30484.
21 A. Bozza, E. E. Coates, T. Incitti, K. M. Ferlin, A. Messina, E. Menna, Y. Bozzi, J. P. Fisher and S. Casarosa, *Biomaterials*, 2014, **35**, 4636–4645.
22 S. Sakai, S. Ito and K. Kawakami, *Acta Biomater.*, 2010, **6**, 3132–3137.
23 S. Sakai, T. Ono, H. Ijima and K. Kawakami, *J. Microencapsulation*, 2000, **17**, 691–699.
24 J. Ma, W. Qi, Y. Xie, W. Wang, W. Yu and X. Ma, *J. Biotechnol.*, 2006, **125**, 242–251.
25 J. Li, Y. Wu, J. He and Y. Huang, *J. Mater. Sci.*, 2016, **51**, 5791–5801.
26 H. Tanaka, M. Matsumura and I. A. Veliky, *Biotechnol. Bioeng.*, 1984, **26**, 53–58.
27 A. Martinsen, I. Storro and G. Skjark-Braek, *Biotechnol. Bioeng.*, 1992, **39**, 186–194.
28 H. Wang, L. Yang and Y. Yang, *Int. J. Biol. Macromol.*, 2025, **292**, 139151.
29 M. Werner, D. Schmoldt, F. Hilbrig, V. Jérôme, A. Raup, K. Zambrano, H. Hübner, R. Buchholz and R. Freitag, *Eng. Life Sci.*, 2015, **15**, 357–367.
30 R. G. Patel, A. Purwada, L. Cerchietti, G. Inghirami, A. Melnick, A. K. Gaharwar and A. Singh, *Cell. Mol. Bioeng.*, 2014, **7**, 394–408.
31 K. Kato, K. Umezawa, D. P. Funeriu, M. Miyake, J. Miyake and T. Nagamune, *BioTechniques*, 2003, **35**(5), 1014–1021.
32 Y. Wang, Y. Li, H. Therien-Aubin, J. Ma, P. W. Zandstra and E. Kumacheva, *Biomicrofluidics*, 2016, **10**, 014110.
33 H. Li, R. F. Leulmi and D. Juncker, *Lab Chip*, 2011, **11**, 528–534.
34 F. Ozawa, K. Ino, T. Arai, J. Ramon-Azcon, Y. Takahashi, H. Shiku and T. Matsue, *Lab Chip*, 2013, **13**, 3128–3135.
35 S. M. George and H. Moon, presented in part at the 2015 28th IEEE International Conference on Micro Electro Mechanical Systems (MEMS), Estoril, Portugal, January, 2015.
36 A. G. Håti, N. B. Arnfinnsdottir, C. Østevold, M. Sletmoen, G. Etienne, E. Amstad and B. T. Stokke, *RSC Adv.*, 2016, **6**, 114830–114842.
37 T. C. Richardson, S. Mathew, J. E. Candiello, S. K. Goh, P. N. Kumta and I. Banerjee, *Biotechnol. J.*, 2018, **13**, 1700099.
38 J. Dusseault, F. A. Leblond, R. Robitaille, G. Jourdan, J. Tessier, M. Menard, N. Henley and J. P. Halle, *Biomaterials*, 2005, **26**, 1515–1522.
39 K. K. Papas, R. C. J. Long, A. Sambanis and I. Constantinidis, *Biotechnol. Bioeng.*, 1999, **66**, 219–230.
40 T. Haque, H. Chen, W. Ouyang, C. Martoni, B. Lawuyi, A. M. Urbanska and S. Prakash, *Biotechnol. Lett.*, 2005, **27**, 317–322.
41 Y. K. Bozhilov, I. Hsu, E. J. Brown and A. C. Wilkinson, *Cells*, 2023, **12**, 896.
42 O. I. Gan, B. Murdoch, A. Larochelle and J. E. Dick, *Blood*, 1997, **90**, 641–650.
43 A. Sauter, D. H. Yi, Y. Li, S. Roersma and S. Appel, *Front. Immunol.*, 2019, **10**, 2352.
44 P. B. Aldo, V. Craveiro, S. Guller and G. Mor, *Am. J. Reprod. Immunol.*, 2013, **70**, 80–86.

